Saudi Pharmaceutical Journal (2012) **20**, 161–170

King Saud University

Saudi Pharmaceutical Journal

www.ksu.edu.sa
www.sciencedirect.com

ORIGINAL ARTICLE

Ethosomes and ultradeformable liposomes for transdermal delivery of clotrimazole: A comparative assessment

Rahul G.S. Maheshwari [a,*], Rakesh K. Tekade [b], Piyoosh A. Sharma [c], Gajanan Darwhekar [a], Abhishek Tyagi [d], Rakesh P. Patel [e], Dinesh K. Jain [a]

[a] *College of Pharmacy, IPS Academy, A.B. Road, Indore 452012, MP, India*
[b] *Ranbaxy Laboratories Limited, Process Development Laboratory (An R&D extension), Industrial Area-III, Dewas 455001, MP, India*
[c] *Department of Pharmaceutical Chemistry, Sri Aurobindo Institute of Pharmacy, Indore, MP, India*
[d] *Institute of Cytology and Preventive Oncology, Indian Council of Medical Research, Noida, UP, India*
[e] *S.K. Patel College of Pharmaceutical Education & Research, Ganpat University, Gujarat, India*

Received 7 July 2011; accepted 22 October 2011
Available online 31 October 2011

KEYWORDS

Anticandidal efficiency;
Atomic force microscopy;
Ethosomes;
Nanocarriers;
Ultradeformable liposomes

Abstract The objective of work was to formulate, evaluate and compare the transdermal potential of novel vesicular nanocarriers: ethosomes and ultradeformable liposomes, containing clotrimazole (CLT), an anti-fungal bioactive. The ethosomal formulation (ET_4) and ultradeformable liposomal (UL) formulation (TT_3) showed highest entrapment 68.73 ± 1.4% and 55.51 ± 1.7%, optimal nanometric size range 132 ± 9.5 nm and 121 ± 9.7 nm, and smallest polydispersity index 0.027 ± 0.011 and 0.067 ± 0.009, respectively. The formulation ET_4 provided enhanced transdermal flux 56.25 ± 5.49 μg/cm^2/h and decreased the lag time of 0.9 h in comparison to TT_3 formulation (50.16 ± 3.84 μg/cm^2/h; 1.0 h). Skin interaction and FT-IR studies revealed greater penetration enhancing effect of ET_4 than TT_3 formulation. ET_4 formulation also had the highest zone of inhibition (34.6 ± 0.57 mm), in contrast to TT_3 formulation (29.6 ± 0.57 mm) and marketed cream formulation (19.0 ± 1.00 mm) against candidal species. Results suggested ethosomes to be the most proficient carrier system for dermal and transdermal delivery of clotrimazole.

* Corresponding author. Tel.: +91 98933 38868; fax: +91 731 5041627.
E-mail address: rahulgsb@yahoo.co.in (R.G.S. Maheshwari).

Peer review under responsibility of King Saud University.
doi:10.1016/j.jsps.2011.10.001

Production and hosting by Elsevier

1. Introduction

Candidiasis, commonly referred to as yeast infection, is a fungal infection of any of the *Candida* species, among them *Candida albicans* being the chief ones (Robin et al., 1995). Clotrimazole, 1-((2-chlorophenyl) diphenylmethyl)-1H-imidazole (CLT) is a broad-spectrum antifungal bioactive like other antimycotic imidazoles that interfere with the ergosterol biosynthesis in a concentration-dependent fashion and thereby causing an alteration of the permeability of cell walls. Its spectrum of efficacy covers all human pathogenic non-invasive fungi including dermatophytes (species of microsporum, trichophyton, and epidermophyton) and yeasts Candida group. Apart from that it is the most commonly prescribed topical antifungal in the United Kingdom for the treatment of tinea pedis. It has a recommended dose or two to three times daily (Steven and James, 1999; Tomohiro et al., 2007; Heinrich, 1978).

The oral administration of the CLT is highly prone toward drug interactions along with low bioavailability and its log *P* value (3.5), and pKa (6.7) permits its transdermal application also (Pandey et al., 2005; Jacobsen et al., 1999; Silva et al., 1998; Khashaba et al., 2000). Although the skin serves as an efficient route for the administration of a number of active ingredients, stratum corneum continues to present drug delivery constraints because of its formidable barrier nature. Molecular weight as well as water solubility of CLT (344.85 D and practically insoluble; respectively) also play a key role that limits the skin delivery of this drug (Mitragotri, 2000; Hashiguchi et al., 1998; Pedersen et al., 1998).

Recently, the techniques like nanoencapsulation, thermosensitive gel formulation, and bio-adhesion, have been successfully engaged to enhance transdermal delivery of CLT (Pandey et al., 2005; Bilensoy et al., 2006; Pavelic et al., 2005).

Modern approaches for drug delivery via skin have resulted in the design of modified liposomes. In this context; nowadays considerable attention has been given to vesicular approaches viz: ultradeformable liposomes (often referred to as 'Transfersomes') and ethosomes. Basically these approaches use the non-toxic and biodegradable, characteristic of phospholipid and for this reason they are able to prolong the half-life of a drug to attain a sustained-release effect. On the other hand, previous studies demonstrated that phospholipids can exhibit their enhancing effect on the skin in the presence of organic solvents such as ethanol (as in the case of ethosomes) and surfactants such as span-80 (as in the case of ultradeformable liposomes). These features make these formulations more advantageous over the liposomes, solutions and creams in terms of skin penetration and therapeutic effects. Moreover, reports on the transdermal delivery of therapeutic agents via ethosomal and ultradeformable liposomal vesicles have been encouraging (Touitou et al., 2000; Jain et al., 2004; Paolino et al., 2005a,b; Elsayed et al., 2006; Paul et al., 1998).

Ultradeformable liposomes consist of phospholipids, an edge activator that increases deformability of the bilayers by destabilizing them and are elastic in nature (Cevc et al., 2002). Ethosomal systems, comprising of phospholipids, ethanol and water, have been reported to improve skin penetration of several drugs (Touitou et al., 2000; Jain et al., 2004; Paolino et al., 2005a,b). The present work thus, emphasizes on the formulation, development and generation of comparative data on transdermal penetration as well as therapeutic efficacy of CLT, thereby, mediating the two novel vesicular approaches.

2. Materials and methods

2.1. Materials

Soybean phosphatidylcholine (Phospholipon–90(H)) (Natterman Phospholipids GMBH, Germany) contained 93.63% phosphatidylcholine. Clotrimazole (Zenith Pharmaceuticals, India) All other chemicals were of HPLC grade and used without further modification.

2.2. Preparation of CLT loaded ethosomes

Ethosomes were prepared by mechanical-dispersion method, as reported and described earlier (Lopez-Pinto et al., 2005; Dubey et al., 2007a,b). Briefly, in a completely dried round bottomed flask (RBF) Phospholipon-90(H) in varying concentrations, (Table 1) was dissolved in a mixture of chloroform and methanol (2:1 v/v). A thin lipid film was then formed on the wall of the RBF using Rotavapour (DB-31355, DICIBEL instruments, India), by maintaining the temperature above the lipid transition temperature (55 ± 2 °C) and the organic solvent was completely evaporated by vacuum, followed by hydration (6 h) with different concentrations (15%, 25%, 35%, 45% w/v of ethanol in water) of hydroethanolic mixture containing CLT (1.0% w/v). The preparations were further subjected to sonication for 3 cycles of 5 min at each 5 min interval.

2.3. Preparation of CLT loaded ultradeformable liposomes

For the preparation of ultradeformable liposomes, mechanical-dispersion method was followed as described earlier (Elsayed et al., 2006; Mahor et al., 2007). Phospholipon-90(H) (85 parts) and the varying parts of Span-80 (5/10/15/20) were dissolved in an organic solvent mixture (methanol and chloroform in the ratio of 2:1) along with CLT (1.0% w/v). A thin lipid film was formed on the wall of the RBF and was hydrated with Phosphate buffer pH 7.4 to make a final suspension concentration of 10 mg/ml. The preparations were further subjected to sonication for 3 cycles of 5 min at each 5 min interval. Furthermore, the ethosomal and ultradeformable liposomal formulations were optimized on the basis of entrapment efficiency and vesicle size (Table 1).

2.4. Size distribution measurement

Vesicle size distributions of ethosomal and UL formulations were measured in two sets of triplicates in a multimodal mode. The technique opted was Dynamic Light Scattering (DLS) using computerized Malvern Autosizer 5002 inspection system (Malvern, UK). Prior to the measurement, formulations were mixed with the PBS, pH 7.4 and the measurements were taken in triplicate.

2.5. Entrapment efficiency

Entrapment efficiencies of ethosomal and ultradeformable liposomes (UL) formulations were measured using Sephadex

Table 1 Composition and optimization parameters of various Ethosomal and UL formulations.

Formulations	Composition		Vesicle size (nm)	PI	%EE
	P:E (%w/v)	S:P (%w/v)			
ET_1	15:3	–	163 ± 13	0.066 ± 0.029	28.4 ± 1.2
ET_2	25:3	–	152 ± 11	0.052 ± 0.021	36.3 ± 2.1
ET_3	35:3	–	144 ± 10	0.050 ± 0.019	48.7 ± 3.4
ET_4	45:3	–	132 ± 9.5	0.279 ± 0.011	68.7 ± 1.4
TT_1	–	5:85	157 ± 8.7	0.087 ± 0.017	32.6 ± 12
TT_2	–	10:85	143 ± 11	0.073 ± 0.013	45.8 ± 3.8
TT_3	–	15:85	121 ± 9.7	0.067 ± 0.009	65.5 ± 1.7
TT_4	–	20:85	184 ± 12	0.095 ± 0.016	42.3 ± 1.4

Note: P:E, Phospholipid:Ethanol (% w/v); S:P, Span-80:Phospholipid: (% w/v); PI, polydispersity index; EE, entrapment efficiency.
Ethosomal formulations (ET_1–ET_4).
Ultradeformable liposomal formulations (TT_1–TT_4).
Values are represented as mean ± SD (n = 3).

G-50 minicolumn centrifugation technique (Fry et al., 1978; Sorensen et al., 1977) For this the formulations that were kept overnight at 4 °C were spun in an ultracentrifuge at 3000 rpm for 1 h (Ultracentrifuge, Hitachi, Singapore). Columns were prepared by allowing 10 g of Sephadex G-50 to swell overnight in 120 ml of 0.9% NaCl solution (Nguyen et al., 1999). Triton X-100 (0.5% w/w) was used as the lysing agent and entrapment efficiency of the drug was calculated using HPLC (Model; LC-10AT_{VP}: Column; Luna 5U C_{18} 100 A; Shimadzu, Kyoto, Japan) using acetonitrile:water (50:50) as a mobile phase at a flow rate of 0.5 ml/min with Twenty microliter injection volume.%. Entrapment efficiency was then calculated using Eq. (1):

$$\text{Entrapment efficiency}(\%) = \frac{\text{Mass of drug in vesicles}}{\text{Mass of drug used in formulation}} \times 100 \quad (1)$$

2.6. Transmission electron microscopy

For Transmission Electron Microscopy (TEM; Philips CM12 Electron Microscope, Netherlands), the samples were negatively stained with a 1% w/v aqueous solution of phosphotungustic acid (PTA) prior to use. Negatively stained samples were examined at an accelerated voltage of 20 kV with a magnification of ×4000.

2.7. Atomic force microscopy (AFM)

In addition to the above mentioned electron microscopic studies, both of the formulations were also analyzed for topography of the sample surface by Digital Instruments, USA Nanoscope E. For AFM study, one drop of each formulation was spread out homogenously on a separate glass piece (4 mm × 4 mm), and imaging was carried out at a scan speed of 10.17 Hz with ×4000 magnification (Ruozi et al., 2007; Sriamornsak et al., 2008).

2.8. Skin permeation studies

Franz diffusion cell was used to determine the in vitro skin permeation of CLT loaded ethosomal and UL formulations. Effective permeation area, receptor cell volume, receptor compartment media and temperature were kept 1.0 cm^2, 10 ml, Phosphate buffer (pH 7.4) and 37 ± 1 °C, respectively. The abdominal portion of a rat (Male Sprague Dawley, 4–5 week old, 100–120 g) was used in the study. After clean shaving, washing and sectioning, the skin was fixed on a receptor compartment (stratum corneum side facing upward into the donor compartment). The ET_4 formulation and TT_3 formulation (250 µl) were applied separately on the donor compartment. Samples (250 µl) were collected at 2, 4, 6, 8, 12, 18, 24 h intervals and analyzed by HPLC (Shimadzu, Model; LC-10AT_{VP}: Column; Luna 5U C_{18} (2) 100 A, Kyoto, Japan). Hydroethanolic CLT solution (1% w/v drug dispersed in 45% hydroethanolic solution) and pure drug solution (1% w/v CLT in water) were also studied to generate comparative data. The cumulative amount of drug permeated per unit area was plotted as a function of time. From this plot, the steady-state permeation rate (Jss) and lag time (h) were calculated from the slope and x intercept of the linear portion, respectively. Experiments were repeated thrice for each formulation (n = 3).

All investigations were performed as per the protocol approved by CSPCSE (Registration No. 465/01/ab/CPCSEA; Letter No. IAEC/IPSA/COP/09/2008).

2.9. Vesicle skin interaction studies

The vesicle skin interaction study was done on the basis of structural changes in stratum corneum, epidermis and dermis. ET_4 and TT_3 formulations were applied topically on the skin of rats (Male Sprague Dawley, 4–5 week old, 90–100 g) for 8 h. After sacrificing the animals by ether inhalation, skin was excised and stored in formalin solution (10% w/v). For the study, thick sections were cut from prepared blocks and subjected to optical microscopy. Similar procedure was followed to prepare control skin section, except the treatment by hydroalcoholic solution instead of ET_4 and TT_3 formulations.

2.10. Evaluation of bilayer fluidity using FT-IR spectroscopy

The whole skin, epidermis and stratum corneum were prepared by the method earlier reported (Panchagnula et al., 2001; Scott et al., 1986). Briefly, the male rat (Sprague–

Dawley, 4–5 week old, 100–120 g) was sacrificed and after hair removal, the dorsal skin was excised, washed with water and the subcutaneous tissue was removed surgically. After washing with phosphate buffer, the skin was defrosted (−20 °C), till used. The epidermis was prepared by treating the skin with 1 M sodium bromide solution in water for 12 h. Stratum corneum was separated from the epidermis using 0.1% w/v trypsin solution in water for 12 h (stratum corneum side facing upward) (Yokomizo, 1996; Scott et al., 1986; Panchagnula et al., 2001). Finally the stratum corneum sheets were dried in a desiccator till completely dried. On the day of the experiment, stratum corneum sheets were treated with ET_4 formulation, TT_3 formulation and hydroethanolic solution (30% ethanol) for 8 h. The treated sheets were dried and investigated by FT-IR spectrophotometer (IR 200; DTGS detector; Thermo Nicolet, USA) between 4000 and 1000 cm^{-1}.

2.11. In vitro anticandidal testing

Standard disk diffusion method as reported earlier (Ingroff, 2007), was followed for in vitro anticandidal testing, and *C. albicans* (ATCC No. 90028) was used as an indicator strain. The culture medium selected for this purpose was Sabouraud Dextrose Agar (SDA; HiMedia Laboratories Pvt. Ltd., Mumbai, India) and the final pH of the medium was kept at 5.6 ± 0.2 to retard the growth of unlike organisms. The medium was sterilized using an autoclave at 121 °C for 20 min. Freshly prepared culture (24 h) was used for inoculum preparation, which was prepared by suspending 1–2 colonies in tubes containing SDA media and 10 ml of sterile saline (0.9% w/v NaCl solution). The turbidity was adjusted to match 0.5 on the McFarland scale (indicating approximately 10^7 cells/ml). Petri dishes (9 cm-diameter) containing medium to a depth of 5 mm were used. The inoculum (0.5 ml) was spread over the surface of SDA media and after appropriate solidification (at 35 ± 2 °C for 10 min), ethosomal formulation (Test I, ET_4) and UL formulation (Test II, TT_3) along with control (marketed cream formulation) (all equivalent to clotrimazole 1% w/v) were applied. The complete experiment was carried out in a sterile area (sterile laminar air flow hood). Finally, the petri plates were incubated at 37 ± 2 °C for 24 h in reverse position. The zone of inhibition (mm of diameter) was calculated (Carrillo-Munoz et al., 2002; Ahmed et al., 1998).

2.12. Statistical analysis

Statistical analysis was performed with Graph Pad Instat Software (version 3.0, Graph Pad Software San Diego, California, USA) using one-way ANOVA followed by Tukey–Kramer multiple comparison test. Difference with $P > 0.05$ was considered statistically insignificant, whereas $P < 0.001$ was considered extremely significant.

3. Results

3.1. % Entrapment efficiency (EE%)

Enormous capability to entrap CLT in lipid bilayer structure was observed with ET_4 formulation (68.73 ± 1.4%), larger than TT_3 formulation (55.51 ± 1.7%). These outcomes elicit the potential of ethosomal carrier system to load as well as deliver CLT at its required therapeutic window.

3.2. Vesicular characterization using TEM

The ethosome and ultradeformable liposome based formulations when visualized by TEM and analyzed by analysis software (Soft Imaging System GmbH, Munster, Germany), exhibited spherical shape mostly with unilamellar pattern, and thereby confirm their vesicular characteristics (Figs. 1A

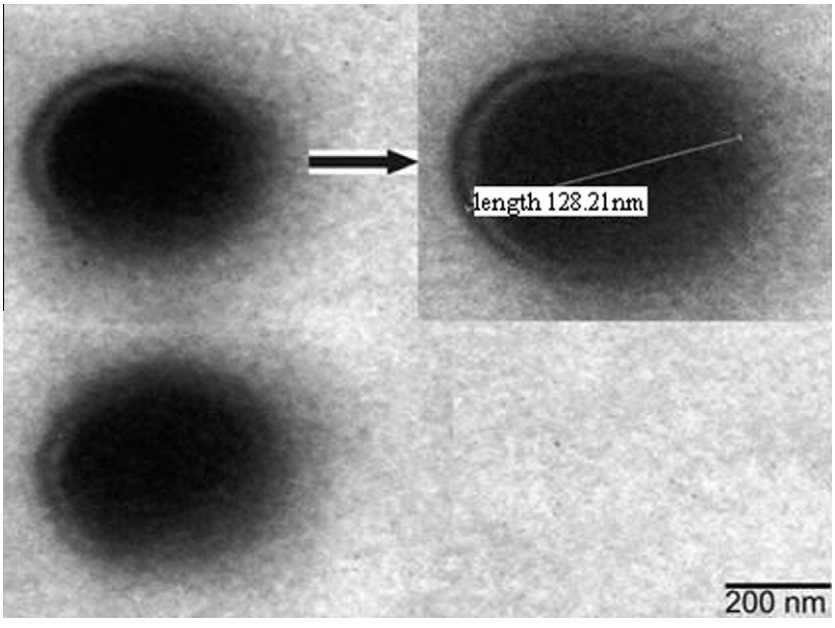

Figure 1A Photomicrograph of ET_4 formulation as seen by TEM (transmission electron microscopy).

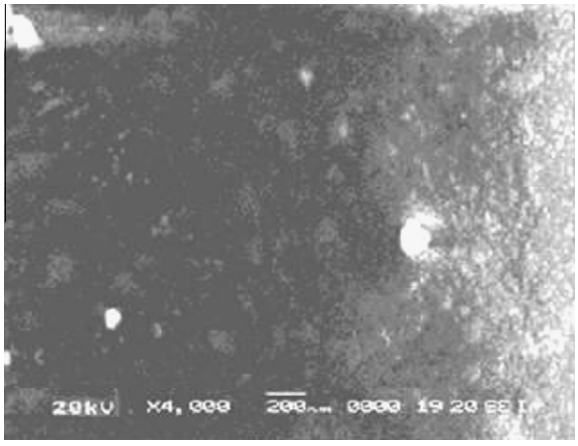

Figure 1B Photomicrograph of TT_3 formulation as seen by TEM (transmission electron microscopy).

and B), with marginal differences, reside in their preparation methods.

3.3. Atomic force microscopy

When the ET_4 formulation was examined by AFM, spherical structure of the small unilamellar vesicles was observed. The size of the ethosomal formulation was measured from the AFM images. The geometric mean diameter and height were 128 ± 10.5 nm and 7.8 ± 1.2 nm respectively. Similarly the geometric mean diameter and height of the TT_3 formulation were found to be 120 ± 9.3 nm and 5.5 ± 1.1 nm respectively (Figs. 2A and B).

3.4. Skin permeation studies

The investigation of transport enhancement ability of ET_4 and TT_3 formulations was measured using the abdominal portion of a rat and the method adapted was Franz diffusion cell measurement. The cumulative amount of CLT permeated per unit area across excised rat skin as the function of time (Fig. 3), steady-state transdermal flux and lag time were determined. The steady-state transdermal flux for CLT loaded ET_4 formulation and TT_3 formulation were observed to be 56.25 ± 5.49 μg/h/cm^2 and 50.16 ± 3.84 μg/h/cm^2, respectively. In addition, the transdermal flux of hydroethanolic solution and plain drug solution was also investigated, and compared with ethosomal and UL formulations, that revealed marked lower flux values ($P < 0.05$) and a higher lag time of 21.25 ± 1.04 μg/h/cm^2, 1.8 h; and 1.20 ± 0.82 μg/h/cm^2, 2.7 h (Table 2).

3.5. Vesicle skin interaction studies

Vesicle skin interaction studies of ET_4 and TT_3 formulations (optimized formulations) exhibit no major alterations in the skin histopathology. However, on application, mild swelling of corneocytes and skin lipid fluidization (penetration

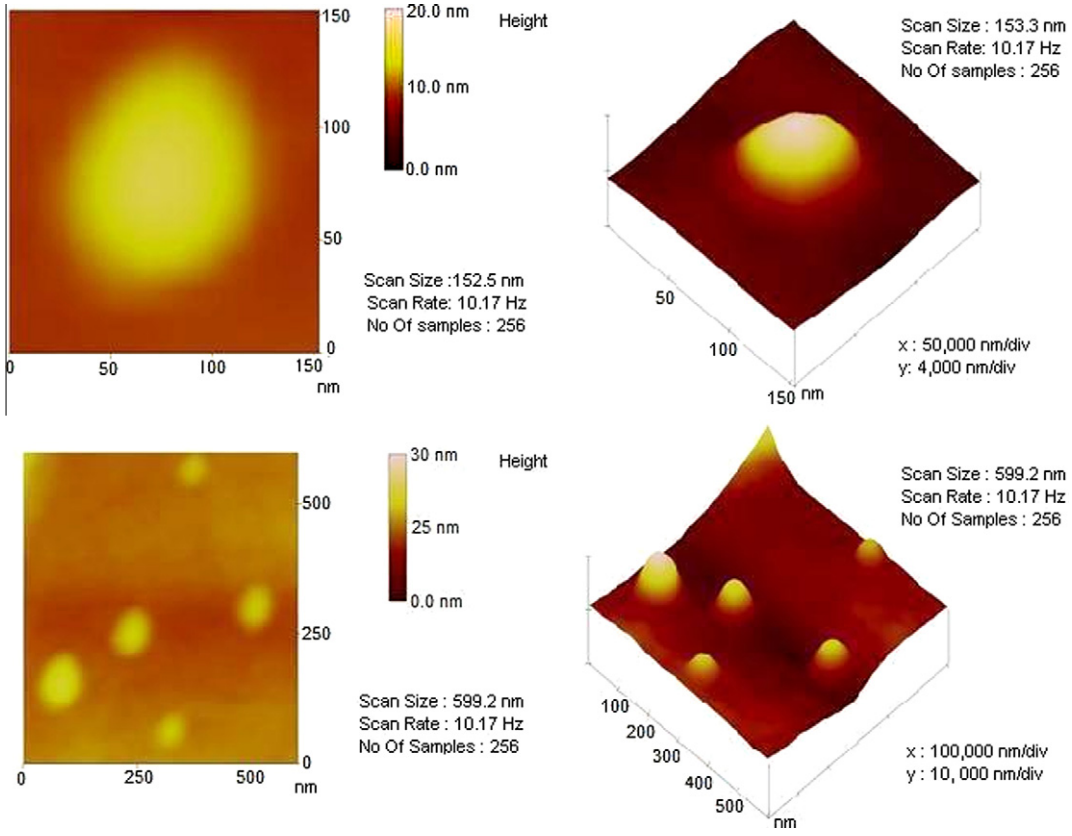

Figure 2A Photomicrographs of ET_4 formulation as seen by AFM (atomic force microscopy).

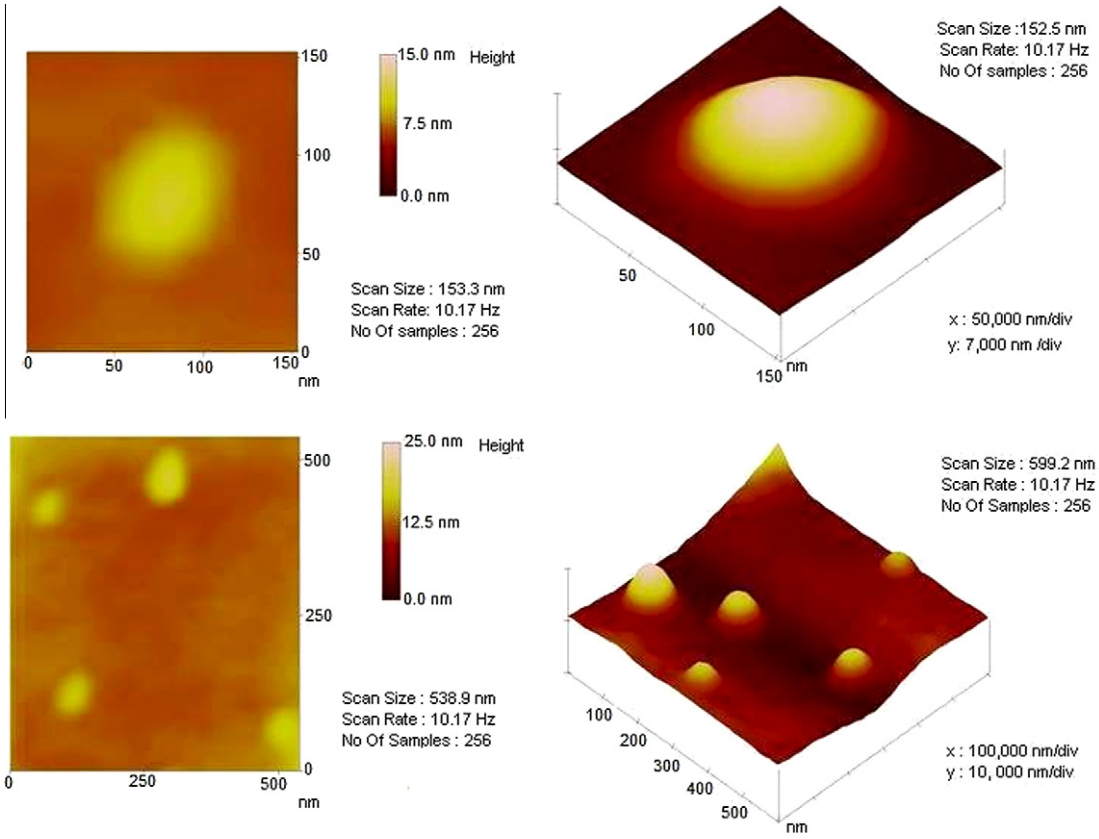

Figure 2B Photomicrographs of TT_3 formulation as seen by AFM (atomic force microscopy).

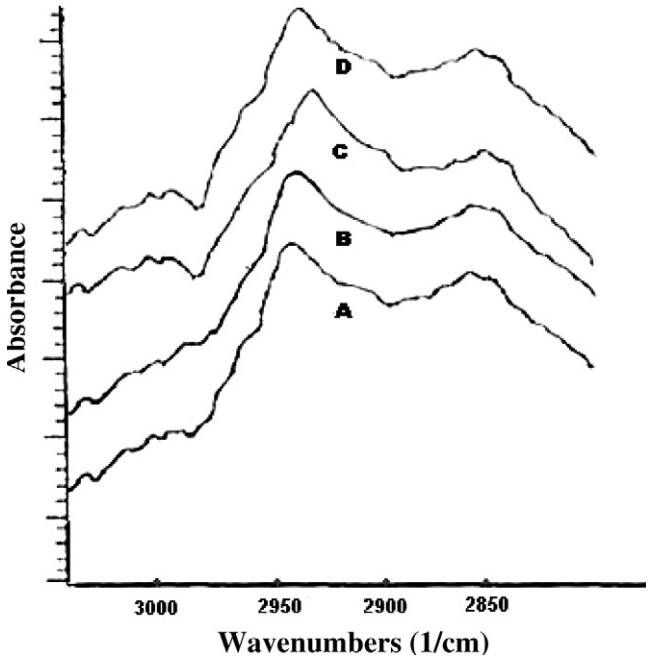

Figure 3 FT-IR spectra of rat skin after 8 h. (A) Untreated skin, (B) Hydroethanolic solution, (C) TT_3 formulation, (D) ET_4 formulation.

pathways) were observed with ET_4 formulation, whereas only slight puffiness was observed in the case of TT_3 formulation. These outcomes revealed the possible mechanisms of skin penetration by these nanocarriers as also explored earlier (Touitou et al., 2000; Cevc et al., 2002; Jain et al., 2004; Paolino et al., 2005a,b; Elsayed et al., 2006; Paul et al., 1998).

3.6. Size distribution measurement

Investigation using Dynamic Light Scattering (DLS) revealed smallest polydispersity index of ET_4 formulation (0.0279 ± 0.019) and TT_3 formulation (0.067 ± 0.009) with optimized vesicle size of 132 ± 9.53 nm and 121.94 ± 9.78 nm, respectively (Table 1). In addition, the vesicle size investigation by TEM and AFM also shows good correlation with zetasizer reports.

3.7. Evaluation of bilayer fluidity using FT-IR spectroscopy

Alteration in the fluidity of stratum corneum was observed by focusing on the region near to 2850 cm^{-1} and 2920 cm^{-1} as shown in Fig. 3. In the case of ET_4 formulation, it may be concluded that the peaks obtained near at 2850 cm^{-1} and 2920 cm^{-1} were due to the C–H symmetric stretching and C-H asymmetric stretching absorbance, with slight alterations, as shown in Table 3.

3.8. In vitro anticandidal testing

The outcomes show greater potential of vesicle systems (in comparison to marketed cream formulation) in inhibiting the

Table 2 Transdermal flux (μg/h/cm^2) and lag time (h) of ET_4, TT_3, Hydroethanolic solution and plain drug solution.

Parameters	ET4	TT3	Hydroethanolic solution (45%)	Plain drug solution (1% CLT)
Transdermal flux (μg/h/cm^2)	56.25 ± 5.49	52.16 ± 3.84	21.25 ± 1.04	1.20 ± 0.82
Lag time (h)	0.9	1.0	1.8	2.7

Values are represented as mean ± SD (n = 3).

Table 3 Alterations on the C–H symmetric and C–H asymmetric stretching absorbance shifts on the acyl chains of stratum corneum lipids upon the application of different formulations.

Skin treatments	C–H symmetric stretching (cm^{-1})	C–H asymmetric stretching (cm^{-1})
Untreated	2850.18 ± 1.21	2920.11 ± 1.11
30% Hydroethanolic solution	2852.38 ± 1.10	2921.76 ± 1.21
TT_3 formulation	2853.56 ± 0.78	2924.42 ± 0.97
ET_4 formulation	2854.89 ± 1.15	2925.12 ± 1.12

Values are represented as mean ± SD (n = 3).

Table 4 *In vitro* anticandidal activity of different formulations using disk diffusion method and *C. albicans* as the test organism.

Formulations	Inhibition zone (mm)			Mean (mm)	SD
	Test I	Test II	Test III		
Control	20	18	19	19.0	1.00
ET_4 (Test I)	34	35	35	34.6	0.57
TT_3 (Test II)	30	29	30	29.6	0.57

Values are represented as mean ± SD (n = 3).

growth of *C. albicans* with a higher zone of inhibitions in a 24 h in vitro anticandidal testing given in Table 4. The average ± SD inhibition zone values of the test formulations (Test I, ET_4 and Test II, TT_3), and control formulation (marketed cream) were found to be 34.6 ± 0.57 mm, 29.6 ± 0.57 mm, and 19.0 ± 1.00 mm, respectively. From the above mentioned results and by comparing the inhibition zone of the test formulations with the control, it was concluded that ET_4 and TT_3 formulations showed much better inhibitions, although the ET_4 and TT_3 formulations were significantly different ($P < 0.001$) from each other, as confirmed using the Student t-test.

4. Discussion

4.1. Formulation, optimization and entrapment efficiency (EE)

We aimed at exploring the opportunities toward transdermal delivery of CLT by modifying lipid membrane composition (Ethosomes and ultradeformable liposomes), with the specific objective to predict surface characteristics and carrier efficiency following topical administration, and thereby comparing the two established approaches.

Initially, formulation/optimization of ethosomal and UL formulations were done on the basis of entrapment efficiency and vesicular size/characteristic analysis, wherein it was found that the ethosomal formulation ET_4 and UL formulation TT_3 possess loading potential of higher order and smallest vesicle size, as shown in the Table 1. Our optimizations are in accordance with the observations of the other scientific groups (Cevc et al., 2002; Lopez-Pinto et al., 2005; Dubey et al., 2007a,b; Mahor et al., 2007).

Furthermore, on comparative assessment of data, a better entrapment efficiency was observed in the case of ET_4 (68.73 ± 1.4%) in comparison to TT_3 (65.51 ± 1.7%) and this could be attributed to better solubility and retentivity of CLT in ethanol present in the ethosomal core, rather than in phosphate buffer pH 7.4, which was engaged as hydration medium during the preparation of TT_3 formulation (Touitou et al., 2000; Jain et al., 2004; Paolino et al., 2005a,b; Elsayed et al., 2006; Paul et al., 1998).

In terms of vesicle size examination, on increasing the concentration of ethanol and surfactant, in the ethosomal and UL formulations, an obvious decrease in vesicle size was observed to a significant level ($P < 0.01$). In the case of ethosomal formulations with ethanol concentration ranging from 15 to 45%, the size of the vesicles decreased with increase in ethanol concentration. The formulation containing 45% ethanol showed smaller size (132 ± 9.5 nm) as compared to that of formulation containing 15% ethanol (163 ± 13 nm). On another side, in the case of UL formulations, the vesicle size of the systems embedded with 5–20 parts of surfactant showed an increase in average vesicle size, but to some degree, as in our case, the formulation containing 15 parts of surfactant showed lowest vesicle size (121 ± 9.7 nm) and the system containing 20 parts of surfactant showed further increases in the vesicle size (184 ± 12 nm). On comparative background, the decrease in vesicle size of ethosomal formulations with increasing ethanol concentration was predominantly assumed to be a function of membrane thickness; wherein considerable reduction in membrane thickness was observed with increase in ethanol concentration ($P < 0.01$). This might be due to the formation of hydrocarbon phase with inter-penetrating properties, an observation experienced by a number of scientific groups (Touitou et al., 2000; Dubey et al., 2007a,b), whereas in the case of UL formulations, increase in span-80 concentration resulted in decrease in vesicle size of the system, might be due to its surface active properties (provides elasticity) and membrane softening/reduction ability. An increased vesicle size (184 ± 12 nm) and decreased entrapment efficiency (42.3 ± 1.4%)

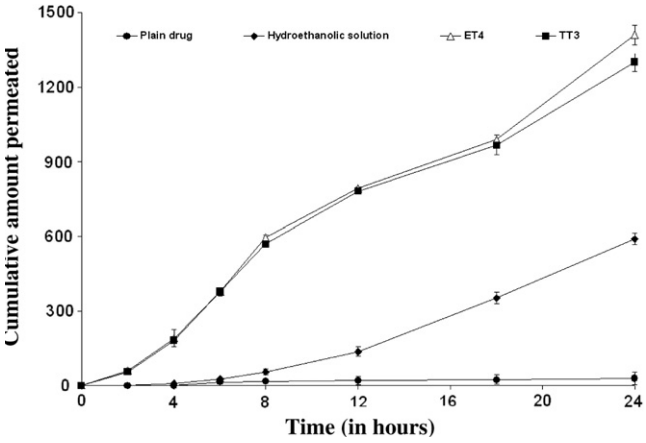

Figure 4 Comparative cumulative amount of CLT permeated from ET_4 formulation, TT_3 Formulation, hydroethanolic solution and plain drug solution in a 24 h study via abdominal rat skin.

was observed in the UL formulation containing 20 parts of surfactant (TT_4), attributing to the reduction in the net charge of the vesicle system (Mahor et al., 2007).

4.2. TEM and AFM measurements

Both the formulations (ET_4 and TT_3) confirm the formation of vesicular structure, spherical shape and mostly unilamellar arrangement, as characterized by TEM. Specifically, ethosomal formulation (ET_4) showed a more imperfect round shape, when compared with UL formulation (TT_3), explaining the fluidizing effect of ethanol, a phenomenon observed earlier (Touitou et al., 2000). The surface morphology and topography revealed by TEM measurements were further confirmed by investigation using AFM. The data (shape, structure, surface morphology and size measurement) obtained using AFM (Fig. 4) clearly indicate regarding the surface properties of formulations.

4.3. Size distribution measurement

Dynamic light scattering, allowed determining the vesicle size as well as the size distribution. The smallest polydispersity index of ET_4 formulation (0.027 ± 0.019) and TT_3 formulation (0.067 ± 0.009) revealed their homogeneous distribution in vesicle systems; and optimized vesicle size of ET_4 formulation (132 ± 9.5 nm) and TT_3 formulation (121.94 ± 9.7 nm) are evidence of their nanometric size range, thereby an overall better permeation profile was obtained. (Table 1).

4.4. Skin permeation studies

Delivery rates of CLT loaded vesicles were investigated by determining the transdermal flux of CLT across excised abdominal rat skin. In comparison to hydroethanolic solution and plain drug solution (21.25 ± 1.04 μg/h/cm^2 1.8 h and 1.20 ± 0.82 μg/h/cm^2, 2.7 h; respectively); ET_4 and TT_3 formulations (56.25 ± 5.49 μg/h/cm2, 0.9 h and 52.16 ± 3.84 μg/h/cm^2, 1.0 h; respectively) attained greater transdermal flux and lower lag time as well. (Paolino et al., 2005a,b; Lodzki et al., 2003; Kirjavainen et al., 1996) On further comparison, the enhanced permeation with ET_4 formulation could be attributed to ethanol content in the ethosomal core (Touitou et al., 2000), whereas, the driving force for the TT_3 formulation entering the skin were xerophobia (tendency to avoid dry surroundings) and the naturally occurring in vivo transcutaneous hydration gradient (Cevc et al., 2002; Dubey et al., 2006; Elsayed et al., 2007; Muzzalupo et al., 2008). Our findings are in good agreement with the earlier reported (Ebtessam et al., 2004; Dubey et al., 2007a,b; Kim et al., 1992).

4.5. Vesicle skin interaction studies

Furthermore, in contrast to TT_3 formulation, accumulations in the top layer of the skin with no significant ultra structural changes were observed only with the skin treated with ET_4 formulation, exploring the partial lipid extraction mechanism and skin lipid fluidization capability of ethanol (Fig. 5A) (Jain et al., 2007), whereas, a slight puffiness of corneocytes, in the case of TT_3 formulation was observed and might be due to the stress-dependent adaptability, which enables them alone to squeeze between the cells in the skin, also indicating the presence of surfactant in the UL formulation (Cevc et al., 2002). Our findings clearly justify the potential of ethanol, to extract and fluidize the skin lipid, which leads to the formation

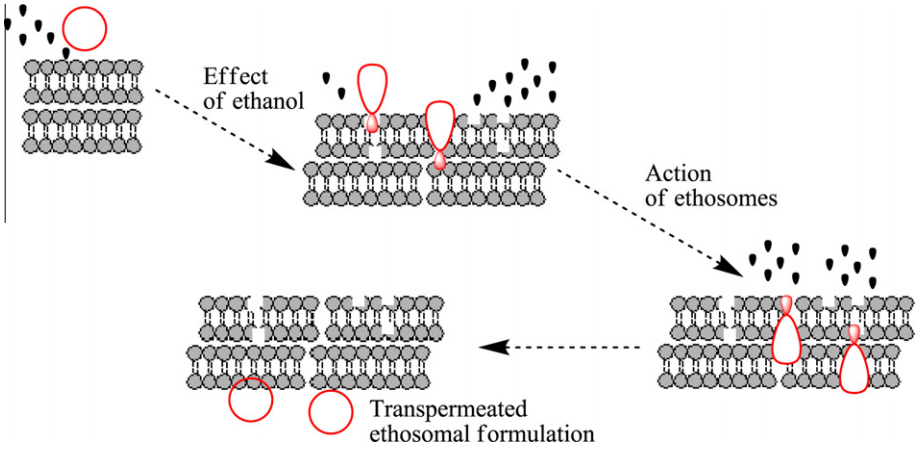

Figure 5A Model schematic for skin delivery from ethosomal system.

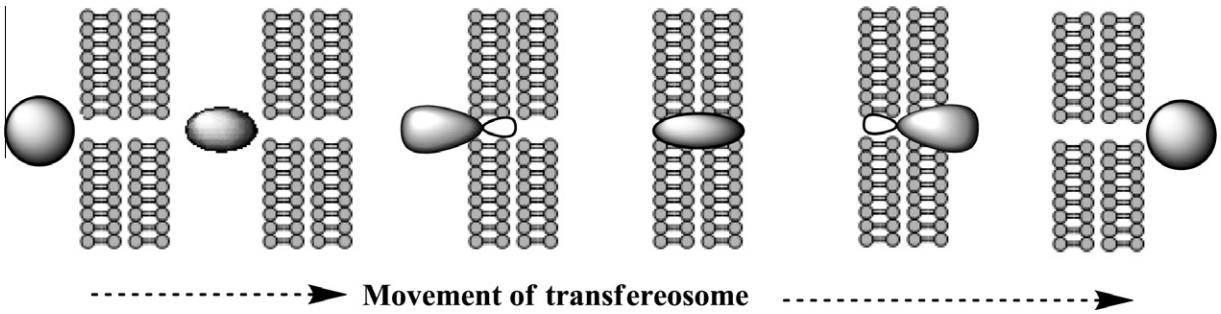

Figure 5B Ultradeformable transfersomes compressing through minute pores in the Stratum corneum.

of small pores, in forms of penetration pathways, further justifying the integrity of ethosomes, over ultradeformable liposomes (Fig. 5B).

4.6. Evaluation of bilayer fluidity using FT-IR spectroscopy

An investigation of lipid bilayer mobility was carried out using FT-IR spectroscopy, using the abdominal portion of rat skin. In comparison to TT_3 formulation, ET_4 formulation showed higher broadening of peaks near 2920 cm^{-1}, which was an indication of an increase in the fluidity of lipid bilayer, probably due to positive alterations in lipid acyl chain with increasing rotational freedom. Furthermore, the push effect (increase in thermodynamic activity due to ethanol evaporation from vesicle system), and pull effect (reduction in barrier properties) of ethanol are responsible for generating an increase of peaks near 2850 cm^{-1} and broadening of peaks near at 2920 cm^{-1}, which could be attributing to enhanced penetration and permeability, as well. These outcomes clearly indicate the disruption of lipid arrangement in lipid bilayer organization, which is lacking in rest of the formulations, probably due to the absence of ethanol. Results are analogous to that reported earlier (Dubey et al).

4.7. In vitro anticandidal testing

In addition, the inhibition zone value of Test I (34.6 ± 0.57 mm), suggested that the ET_4 formulation exhibited better in vitro anticandidal activity against *C. albicans* in comparison with Test II (29.6 ± 0.57 mm) and control (19.0 ± 1.00 mm) formulations. It was found that the test I was significantly different from test II and control ($P < 0.01$ in both cases), So it can be concluded that the ethanol containing formulation exhibited better anticandidal activity than the surfactant containing formulation, probably due to the extra potential of ethanol to kill organisms by denaturing their proteins and dissolving their lipids, apart from skin fluidization and penetration (McDonnell and Russell, 1999). From this study, it can be concluded that the ethanol containing formulation is the better carrier system and is a therapeutically promising candidate for the efficient skin delivery of CLT, over surfactant based formulation.

5. Conclusion

Our results of transdermal flux, bilayer fluidity measurement, entrapment efficiency and in vitro anticandidal testing suggest better aptness of CLT with ethosomal formulation, instead of UL formulation, might be due to greater solubility, retentivity, and adaptability in lipid bilayers consisting of ethanol. This research in particular may shed new light toward ongoing research toward the development of effective formulation for enhanced transdermal delivery particularly in the case of skin ailments like Acneiform eruptions, Chronic blistering, Dermatitis, Epidermal nevi, neoplasms, cysts, Parasitic infestations, Lichenoid eruptions, Mucinoses, Pruritic, Psoriasis etc.

Acknowledgements

The authors are highly grateful to The All India Institute of Medical Sciences, New Delhi, India for providing TEM facility. The authors are also thankful to Dr. D. M. Phase and Mr. Vinay Ahire, UGC-DAE CSR, Indore for providing SEM facility. The authors also acknowledge Dr. V. Ganesan, UGC-DAE CSR, Indore for providing AFM facility. The acknowledgement also goes to Dr. U.K. Garg and Mr. Swapnil Jagtap (College of Veterinary sciences, Mhow, India) for their expertise support for in vivo operations.

References

Ahmed, M.O., El-Gibaly, I., Ahmed, S.M., 1998. Effect of cyclodextrins on the physicochemical properties and antimycotic activity of clotrimazole. Int. J. Pharm. 171, 111–121.

Bilensoy, E., Rouf, M.A., Vural, I., Hincal, A., 2006. Thermosensitive vaginal gel formulation for the controlled release of clotrimazole via complexation to beta-cyclodextrin. J. Contr. Rel. 116, 107–109.

Carrillo-Munoz, A.J., Brio, S., Alonso, R., Valle, O.D., Santos, P., Quindos, G., 2002. Ciclopiroxolamine: in-vitro antifungal activity against clinical yeast isolates. Int. J. Antimicrob. Agents 20, 375–379.

Cevc, G., Schatzlein, A., Richardsen, H., 2002. Ultradeformable lipid vesicles can penetrate the skin and other semi-permeable barriers unfragmented: Evidence from double label CLSM experiments and direct size measurements. Biochim. Biophys. Acta Biomembr. 1564, 21–30.

Dubey, V., Mishra, D., Asthana, A., Jain, N.K., 2006. Transdermal delivery of a pineal hormone: melatonin via elastic liposomes. Biomaterials 27, 3491–3496.

Dubey, V., Mishra, D., Dutta, T., Nahar, M., Saraf, D.K., Jain, N.K., 2007a. Dermal and transdermal delivery of an anti-psoriatic agent via ethanolic liposomes. J. Contr. Rel. 123, 148–154.

Dubey, V., Mishra, D., Jain, N.K., 2007b. Melatonin loaded ethanolic liposomes: Physicochemical characterization and enhanced transdermal delivery. Eur. J. Pharm. Biopharm. 67, 398–405.

Ebtessam, A.E., Michael, C.B., Brian, W., 2004. Electrically assisted skin delivery of liposomal estradiol; phospholipid as damage retardant. J. Contr. Rel. 9, 535–546.

Elsayed, M.M., Abdallah, O.Y., Naggar, V.F., Khalafalla, N.M., 2006. Deformable liposomes and ethosomes: mechanism of enhanced skin delivery. Int. J. Pharm. 322, 60–66.

Elsayed, M.M., Abdallah, O.Y., Nagga, V.F., Khalafallah, N.M., 2007. Lipid vesicles for skin delivery of drugs: Reviewing three decades of research. Int. J. Pharm. 332, 1–16.

Fry, D.W., White, J.C., Goldman, I.D., 1978. Rapid separation of low molecular weight solutes from liposomes without dilution. J. Anal. Biochem. 90, 809–815.

Hashiguchi, T., Kodama, A., Ryu, A., Otagiri, M., 1998. Retention capacity of topical imidazole antifungal agents in the skin. Int. J. Pharm. 161, 195–204.

Heinrich, B., 1978. Analogy in the mode of action of fluotrimazole and clotrimazole in Ustilago avenae Pestic. Biochem. Physiol. 8, 15–25.

Ingroff, A.E., 2007. Standardized disk diffusion method for yeasts. Clin. Microbiol. Newsletter 29, 97–100.

Jacobsen, J., Bjerregaard, S., Pedersen, M., 1999. Cyclodextrin inclusion complexes of antimycotics intended to act in the oral cavity drug supersaturation, toxicity on TR146 cells and release from a delivery system. Eur. J. Pharm. Biopharm. 48, 217–224.

Jain, S., Maheshwari, M., Bhadra, D., Jain, N.K., 2004. Ethosomes: a novel vesicular carrier for enhanced transdermal delivery of an anti-HIV agent. Ind. J. Pharm. Sci. 66, 72–81.

Jain, S., Tiwary, A.K., Sapra, B., Jain, N.K., 2007. Formulation and Evaluation of Ethosomes for Transdermal Delivery of Lamivudine. AAPS PharmSciTech. 8, 249–257.

Khashaba, P.Y., El-Shabouri, S.R., Emara, K.M., Mohamed, A.M., 2000. Analysis of some antifungal drugs by spectrophotometric and spectrofluorimetric methods in different pharmaceutical dosage forms. J. Pharm. Biomed. Ana. 22, 363–376.

Kim, Y.K., Ghanem, A.H., Mahmoud, H., Higuchi, W.I., 1992. Short chain alkanols as transport enhancers for lipophilic and polar/ionic permeants in hairless mouse skin: mechanism(s) of action. Int. J. Pharm. 80, 17–31.

Kirjavainen, M., Urtti, A., Jääskeläinen, I., et al., 1996. Interaction of liposomes with human skin in vitro-the influence of lipid composition and structure. Biochim. Biophys. Acta 1304, 179–189.

Lodzki, M., Godin, B., Rakou, L., Mechoulam, R., Gallily, R., Touitou, E., 2003. Cannabidol-transdermal delivery and anti-inflammatory effect in murine model. J. Control. Release 93, 377–387.

Lopez-Pinto, J.M., González-Rodríguez, M.L., Rabasco, A.M., 2005. Effect of cholesterol and ethanol on dermal delivery from DPPC liposomes. Int. J. Pharm. 298, 1–12.

Mahor, S., Rawat, A., Dubey, P.K., Gupta, P.K., Khatri, K., Goyal, A.K., Vyas, S.P., 2007. Cationic transfersomes based topical genetic vaccine against hepatitis B. Int. J. Pharm. 340, 13–19.

McDonnell, G., Russell, A.D., 1999. Antiseptics and disinfectants: activity, action, and resistance. Clin. Microbiol. Rev. 12, 147–179.

Mitragotri, S., 2000. Synergistic effect of enhancers for transdermal drug delivery. Pharm. Res. 17, 1354–1359.

Muzzalupo, R., Tavano, L., Trombino, S., Cassano, R., Picci, N., Mesa, C.L., 2008. Niosomes from α,ω-trioxyethylene-bis(sodium 2-dodecyloxy-propylenesulfonate): Preparation and characterization. Colloid Surf. B: Biointerfaces 64, 200–207.

Nguyen, T., McNamara, K.P., Rosenzweig, Z., 1999. Optochemical sensing by immobilizing fluorophore-encapsulating liposomes in sol–gel thin films. Anal. Chim. Acta 400, 45–54.

Panchagnula, R., Salve, P.S., Thomas, N.S., Jain, A.K., Ramarao, P., 2001. Transdermal delivery of naloxone: effect of water, propylene glycol, ethanol and their binary combinations on permeation through rat skin. Int . J. Pharm. 219, 95–105.

Pandey, R., Ahmad, Z., Sharma, S., Khuller, G.K., 2005. Nano-encapsulation of azole antifungals: Potential applications to improve oral drug delivery. Int. J. Pharm. 301, 268–276.

Paolino, D., Lucania, G., Mardente, D., Alhaique, F., Fresta, M., 2005a. Ethosomes for skin delivery of ammonium glycyrrhizinate: in vitro permeation through human skin and in vivo skin anti-inflammatory activity of human volunteers. J. Contr. Rel. 106, 99–110.

Paolino, D., Lucania, G., Mardente, D., Alhaique, F., Fresta, M., 2005b. Ethosomes for skin delivery of ammonium glycyrrhizinate: in vitro percutaneous permeation through human skin and in vivo skin anti-inflammatory activity on human volunteers. J. Contr. Rel. 106, 99–110.

Paul, A., Cevc, G., Bachhawat, B.K., 1998. Transdermal immunisation with an integral membrane component, gap junction protein, by means of ultradeformable drug carriers, transfersomes. Vaccine 16, 188–195.

Pavelic, Z., Basnet, N.S., Jalsenjak, I., 2005. Characterization and in vitro evaluation of bioadhesive liposome gels for local therapy of vaginitis. Int. J. Pharm. 301, 140–148.

Pedersen, M., Bjerregaard, S., Jacobsen, J., Sorensen, A.M., 1998. A genuine clotrimazole γ-cyclodextrin inclusion complex-isolation, antimycotic activity, toxicity and an unusual dissolution rate. Int. J. Pharm. 176, 121–131.

Robin, A., Mei-Ling, T., Onderdonk, A., 1995. Effect of *Candida albicans* infection and clotrimazole treatment on vaginal microflora in-vitro. Obstet. Gynecol. 86, 925–930.

Ruozi, B., Tosi, G., Leo, E., Vandelli, M.A., 2007. Application of atomic force microscopy to characterize liposomes as drug and gene carriers. Talanta 73, 12–22.

Scott, R.C., Walker, M., Dugard, P.H., 1986. In-vitro percutaneous absorption experiments. A technique for production of intact epidermal membrane from rat skin. J. Soc. Cosmet. Chem. 37, 35–41.

Silva, H., Gibbs, A., Arguedas, J., 1998. A comparison of fluconazole with ketoconazole, itraconazole, and clotrimazole in the treatment of patients with pityriasis versicolor. Curr. Therap. Res. 59, 203–214.

Sorensen, E.N., Weisman, G., Vidaver, G.A., 1977. A Sephadex column for measuring uptake and loss of low molecular weight solutes from small vesicles. Anal. Biochem. 82, 376–384.

Sriamornsak, P., Thirawong, N., Nunthanid, J., Puttipipatkhachorn, S., Thongborisute, J., Takeuchi, H., 2008. Atomic force microscopy imaging of novel self-assembling pectin–liposome nanocomplexes. Carbohydrate Polymers 71, 324–329.

Steven, L., James, T., 1999. Noncompetitive mixed-type inhibition of rainbow trout CYP1A catalytic activity by clotrimazole, Comparative Biochemistry and Physiology. Endocrinol 122, 205–210.

Tomohiro, M., Toshihisa, B., Keisuke, O., Yoko, S., Midori, M., Hiroko, M., Yasuo, O., 2007. Clotrimazole, an antifungal drug possessing diverse actions, increases membrane permeation of cadmium in rat thymocytes. Toxicol. In Vitro 21, 1505–1512.

Touitou, E., Dayan, N., Bergelson, L., Godin, B., Eliaz, M., 2000. Ethosomes-novel vesicular carriers for enhanced delivery: characterization and skin penetration properties. J. Contr. Rel. 65, 403–418.

Yokomizo, Y., 1996. Effect of phosphatidylcholine on the percutaneous penetration of drugs through the dorsal skin of guinea pigs in vitro; and analysis of the molecular mechanism, using attenuated total reflectance-Fourier transform infrared (ATR-FTIR) spectroscopy. J. Contr. Rel. 42, 249–262.